

# A Convergent and Efficient Deep Q Network Algorithm

**Zhikang T. Wang**

Department of Physics and  
Institute for Physics of Intelligence,  
University of Tokyo  
wang@cat.phys.s.u-tokyo.ac.jp

**Masahito Ueda**

Department of Physics and  
Institute for Physics of Intelligence,  
University of Tokyo  
RIKEN Center for Emergent Matter Science (CEMS)  
ueda@cat.phys.s.u-tokyo.ac.jp

## Abstract

Despite the empirical success of the deep Q network (DQN) reinforcement learning algorithm and its variants, DQN is still not well understood and it does not guarantee convergence. In this work, we show that DQN can diverge and cease to operate in realistic settings. Although there exist gradient-based convergent methods, we show that they actually have inherent problems in learning behaviour and elucidate why they often fail in practice. To overcome these problems, we propose a convergent DQN algorithm (*C-DQN*) by carefully modifying DQN, and we show that the algorithm is convergent and can work with large discount factors ( $\sim 0.9998$ ). It learns robustly in difficult settings and can learn several difficult games in the *Atari 2600* benchmark where DQN fail, within a moderate computational budget. Our codes have been publicly released and can be used to reproduce our results.<sup>1</sup>

## 1 Introduction

With the development of deep learning, reinforcement learning (RL) that utilizes deep neural networks has demonstrated great success recently, finding applications in various fields including robotics, games, and scientific research (Levine et al., 2018; Berner et al., 2019; Fösel et al., 2018; Wang et al., 2020). One of the most efficient RL strategy is Q-learning (Watkins, 1989), and the combination of Q-learning and deep learning leads to the DQN algorithms (Mnih et al., 2015; Hessel et al., 2018), which hold records on many difficult RL tasks (Badia et al., 2020). However, unlike supervised learning, Q-learning, or more generally temporal difference (TD) learning, does not guarantee convergence when function approximations such as neural networks are used, and as a result, their success is often empirical and relies heavily on the hyperparameter tuning.

The divergence problem was pointed out decades ago by the pioneering works of Baird (1995) and Tsitsiklis and Van Roy (1997), and it has been empirically investigated for DQN by Van Hasselt et al. (2018). We also observe the divergence of DQN in our experiments in a realistic setting, as shown in Fig. 6. The divergence, or non-convergence, often shows up as instability in practice and places significant obstacles to the application of DQN to complicated real-world tasks. It makes training with deeper neural networks more difficult, limits the time horizon for planning, and makes the results sometimes unstable and highly dependent on the tuned hyperparameters. This is not satisfactory especially for scientific applications, where convergence and generality are desired. Although gradient-based convergent methods have also been proposed (Sutton et al., 2009; Bhatnagar et al., 2009; Feng et al., 2019; Ghiassian et al., 2020), they cannot straightforwardly be used with neural networks, and they often show worse performance than TD methods and DQN.

<sup>1</sup><https://github.com/Z-T-WANG/ConvergentDQN>

In this work we show that the above-mentioned gradient-based methods actually have inherent problems in their learning behaviour, and as an alternative, we propose a convergent DQN (*C-DQN*) algorithm by modifying the loss in DQN so as to make it non-increasing. In Sec. 2 we present the background. In Sec. 3 we discuss the inefficiency issues in the gradient-based methods and demonstrate using toy problems, and in Sec. 4 we propose our C-DQN and show its theoretical convergence. In Sec. 5 we show the results of C-DQN on the *Atari 2600* benchmark (Bellemare et al., 2013). In Sec. 6 we discuss related works and in Sec. 7 we present the conclusion and future perspectives.

## 2 Background

Reinforcement learning considers a Markov decision process (MDP), where the state  $s_t$  of an environment at time step  $t$  makes a transition to a next state  $s_{t+1}$  conditioned on the action of the agent  $a_t$  at time step  $t$ , producing a reward  $r_t$  that depends on the states. The process can terminate at terminal states  $s_T$ , and it can be probabilistic or deterministic. The goal is to find a policy  $\pi(s)$  to determine all the actions  $a_{t+i} \sim \pi(s_{t+i})$  in order to maximize the return  $\sum_{i=0}^{T-t} r_{t+i}$ , i.e. the sum of rewards. For convenience, a discounted return  $\sum_{i=0}^{T-t} \gamma^i r_{t+i}$  with the discount factor  $\gamma < 1$  but close to 1 is often considered instead, so that rewards far into the future are ignored and that the expression is convergent for  $T \rightarrow \infty$ . Following a policy  $\pi$ , the value function is defined as the expected return for a state  $s_t$ , and the Q function as the expected return for a state-action pair:

$$V_\pi(s_t) = \mathbb{E}_{a_t \sim \pi(s_t), \{(s_{t+i}, a_{t+i})\}_{i=1}^{T-t}} \left[ \sum_{i=0}^{T-t} \gamma^i r_{t+i} \right], \quad Q_\pi(s_t, a_t) = \mathbb{E}_{\{(s_{t+i}, a_{t+i})\}_{i=1}^{T-t}} \left[ \sum_{i=0}^{T-t} \gamma^i r_{t+i} \right], \quad (1)$$

with  $a_{t+i} \sim \pi(s_{t+i})$ . When the Q function is maximized, we say that the policy is optimal and denote the Q function and the policy by  $Q^*$  and  $\pi^*$ . The optimality implies that  $Q^*$  satisfies the Bellman equation (Sutton and Barto, 2018)

$$Q^*(s_t, a_t) = r_t + \gamma \mathbb{E}_{s_{t+1}} \left[ \max_{a'} Q^*(s_{t+1}, a') \right]. \quad (2)$$

The policy  $\pi^*$  is deterministic and is greedy with respect to  $Q^*$ , i.e.  $\pi^*(s) = \operatorname{argmax}_{a'} Q^*(s, a')$ . Q-learning uses this recursive relation to learn  $Q^*$ . In this work we focus on the deterministic case of state transitions and drop the notation  $\mathbb{E}_{s_{t+1}} [\cdot]$  wherever appropriate.

When the space of state-action pairs is small and finite, we can write down the values of the Q function for all possible state-action pairs into a table, and iterate the procedure

$$\Delta Q(s_t, a_t) = \alpha \left( r_t + \gamma \max_{a'} Q(s_{t+1}, a') - Q(s_t, a_t) \right), \quad (3)$$

where  $\alpha$  is the learning rate. This is called Q-table learning and it guarantees convergence to  $Q^*$ . When the space of  $(s, a)$  is large and Q-table learning is impossible, function approximation is used instead, using parameters  $\theta$  representing the Q function as  $Q_\theta$ . The simplest learning rule for  $\theta$  is

$$\Delta \theta = \alpha \nabla_\theta Q_\theta(s_t, a_t) \left( r_t + \gamma \max_{a'} Q_\theta(s_{t+1}, a') - Q_\theta(s_t, a_t) \right), \quad (4)$$

which can be interpreted as trying to modify the value of  $Q_\theta(s_t, a_t)$  so that  $Q_\theta(s_t, a_t)$  approaches the target value  $r_t + \gamma \max_{a'} Q_\theta(s_{t+1}, a')$ . However, it is clear that this iteration may not converge at all, because the term  $\max_{a'} Q_\theta(s_{t+1}, a')$  is also  $\theta$ -dependent and may move together with  $Q_\theta(s_t, a_t)$ . Specifically, it results in divergence when the value of  $\max_{a'} Q_\theta(s_{t+1}, a')$  is not constrained by other means and  $\gamma \nabla_\theta Q_\theta(s_t, a_t) \cdot \nabla_\theta \max_{a'} Q_\theta(s_{t+1}, a') > \|\nabla_\theta Q_\theta(s_t, a_t)\|^2$  is always satisfied. This can be a serious issue for real problems, because the adjacent states  $s_t$  and  $s_{t+1}$  are often similar and  $\nabla_\theta Q_\theta(s_t, a_t)$  can be close to  $\nabla_\theta Q_\theta(s_{t+1}, a')$ .

The DQN algorithm uses a deep neural network with parameters  $\theta$  as  $Q_\theta$  (Mnih et al., 2015), and to stabilize the learning, it introduces a target network with parameters  $\tilde{\theta}$ , and replace the term  $\max_{a'} Q_\theta(s_{t+1}, a')$  by  $\max_{a'} Q_{\tilde{\theta}}(s_{t+1}, a')$ , so that the target value  $r_t + \gamma \max_{a'} Q_{\tilde{\theta}}(s_{t+1}, a')$  does not move together with  $Q_\theta$ . The target network  $\tilde{\theta}$  is then updated by copying from  $\theta$  once for every few thousand iterations of  $\theta$ . This strategy has shown great empirical success, and together with the use of offline sampling and adaptive optimizers, it can be used to learn various tasks including

real simple video games and simulated robotic control (Mnih et al., 2015; Lillicrap et al., 2015). Nevertheless, the introduction of the target network  $\tilde{\theta}$  was not well-principled, and it does not fully resolve the non-convergence issue. As a result, DQN may require a significant amount of hyperparameter tuning in order to work on a new task, and when the task is difficult, the instability can be hard to diagnose or remove. In an attempt to solve this problem, Durugkar and Stone (2017) considered only updating  $\theta$  in a direction that is perpendicular to  $\nabla_{\theta} \max_{a'} Q_{\theta}(s_{t+1}, a')$ ; however, this is not satisfactory in general and can lead to poor performance, as shown in Pohlen et al. (2018).

Another way of approaching this problem is to consider the mean squared Bellman error (MSBE), which is originally proposed by Baird (1995) and called the *residual gradient* (RG) algorithm. The Bellman error, or Bellman residual, TD error, is given by  $\delta_t(\theta) := r_t + \gamma \max_{a'} Q_{\theta}(s_{t+1}, a') - Q_{\theta}(s_t, a_t)$ . Given observed state-action data,  $\delta_t$  is a function of  $\theta$  alone, and we can minimize the MSBE loss

$$L_{MSBE}(\theta) := \mathbb{E} \left[ |\delta(\theta)|^2 \right] = \frac{1}{|\mathcal{S}|} \sum_{(s_t, a_t, r_t, s_{t+1}) \in \mathcal{S}} \left| Q_{\theta}(s_t, a_t) - r_t - \gamma \max_{a'} Q_{\theta}(s_{t+1}, a') \right|^2, \quad (5)$$

where  $\mathcal{S}$  is the dataset, and the loss is minimized via gradient descent. If  $L_{MSBE}$  becomes zero, we have  $\delta_t \equiv 0$  and the Bellman equation is satisfied, implying  $Q_{\theta} = Q^*$ . With a fixed dataset  $\mathcal{S}$ , by definition the learning process should converge, as long as the optimization of the loss converges. When used with a neural network, this strategy is known as the neural fitted Q iteration (NFQ) (Riedmiller, 2005), and it is successfully demonstrated on small toy tasks. There have also been many improvements on this strategy including Sutton et al. (2008, 2009); Bhatnagar et al. (2009); Dai et al. (2018); Feng et al. (2019); Ghiassian et al. (2020); Touati et al. (2018), and they are often referred to as gradient-TD methods. Many of them have focused on how to deal with the evaluation of the expectation term in Eq. (2). Unfortunately, most of these methods often do not work well on difficult problems, and few of them have been successfully demonstrated on standard RL benchmarks, especially the *Atari 2600* benchmark. In the following we will refer to the strategy of minimizing  $L_{MSBE}$  as the RG algorithm, or RG learning.

### 3 Inefficiency of minimizing the MSBE

#### 3.1 Ill-conditionness of the loss

In the following we show that using Eq. (5) as the loss to minimize does not lead to efficient reinforcement learning in general, and we demonstrate using toy deterministic tabular problems, for which all the gradient-TD methods are supposed to reduce to the form of RG ideally. Consider the tabular case, where the Q function values for different state-action pairs can be treated as independent variables. Suppose we have a trajectory of experience  $\{(s_t, a_t, r_t)\}_{t=0}^{N-1}$  obtained by following the greedy policy with respect to  $Q$ , i.e.  $a_t = \arg\max_{a'} Q(s_t, a')$ , and  $s_N$  is a terminal state. Taking  $\gamma = 1$ , the MSBE loss is given by

$$L_{MSBE} = \frac{1}{N} \left[ \sum_{t=0}^{N-2} (Q(s_t, a_t) - r_t - Q(s_{t+1}, a_{t+1}))^2 + (Q(s_{N-1}, a_{N-1}) - r_{N-1})^2 \right]. \quad (6)$$

If we write  $Q_t := Q(s_t, a_t)$ , despite its simple quadratic form, the Hessian matrix of  $L_{MSBE}$  regarding variables  $\{Q_t\}_{t=0}^{N-1}$  is actually ill-conditioned, and therefore does not allow efficient gradient descent optimization. The condition number  $\kappa$  of the hessian is defined by  $\kappa := \frac{|\lambda_{\max}|}{|\lambda_{\min}|}$ , where  $\lambda_{\max}$  and  $\lambda_{\min}$  are the largest and smallest eigenvalues. It can be numerically found that  $\kappa$  of the Hessian of  $L_{MSBE}$  in Eq. (6) grows as  $O(N^2)$ . To find an analytic expression, we add an additional term  $Q^2(s_0, a_0)$  to  $L_{MSBE}$ , and the Hessian matrix is

$$\begin{pmatrix} 4 & -2 & & \\ -2 & 4 & \ddots & \\ & \ddots & \ddots & -2 \\ & & -2 & 4 \end{pmatrix}_{N \times N}, \quad (7)$$

of which the eigenvectors have the form of standing waves, given by  $(\sin \frac{k\pi}{N+1}, \sin \frac{2k\pi}{N+1}, \dots, \sin \frac{Nk\pi}{N+1})^T$  for  $k \in \{1, 2, \dots, N\}$ , and the eigenvalues are given by  $4 - 4 \cos \frac{k\pi}{N+1}$ . Therefore, we obtain  $\kappa = \frac{1 + \cos \frac{\pi}{N+1}}{1 - \cos \frac{\pi}{N+1}} \sim O(N^2)$ .

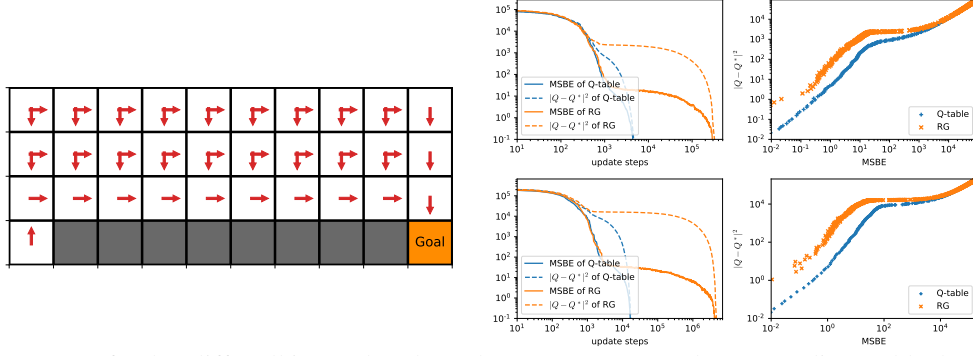


Figure 1: Left: the cliff walking task, where the agent can move between adjacent blocks and is supposed to go to the lower right corner and avoid the grey region. The red arrows show the optimal policy. In this example the system has the height of 4 and the width of 10. Right: results of learning the cliff walking task in a tabular setting, using randomly sampled state-action pair data. The upper plots show the result with width 10 and  $\gamma = 0.9$ , and the lower show width 20 and  $\gamma = 0.95$ .  $|Q - Q^*|^2$  is the squared distance between the learned Q function and the optimal  $Q^*$ .<sup>3</sup> Both Q-table learning and RG use the learning rate of 0.5, averaged over 10 repeated runs.

With  $\gamma < 1$ , if the states form a cycle, i.e. if  $s_{N-1}$  goes back to  $s_0$ , the loss becomes  $L_{MSBE} = \frac{1}{N} [\sum_{t=0}^{N-2} (Q_t - r_t - \gamma Q_{t+1})^2 + (Q_{N-1} - r_{N-1} - \gamma Q_0)^2]$ . The Hessian matrix is cyclic and the eigenvectors have the form of periodic waves:  $(\sin \frac{2k\pi}{N}, \sin \frac{4k\pi}{N}, \dots, \sin \frac{2Nk\pi}{N})^T$  and  $(\cos \frac{2k\pi}{N}, \cos \frac{4k\pi}{N}, \dots, \cos \frac{2Nk\pi}{N})^T$ , with eigenvalues  $2(1 + \gamma^2) - 4\gamma \cos \frac{2k\pi}{N}$  (with some double counting). At the limit of  $N \rightarrow \infty$ , we have  $\kappa = \frac{(1+\gamma)^2}{(1-\gamma)^2} \sim O\left(\frac{1}{(1-\gamma)^2}\right)$ . By interpreting  $\frac{1}{1-\gamma}$  as the effective time horizon, or the effective size of the problem, we see that  $\kappa$  is quadratic in the size of the problem, which is the same as its dependence on  $N$  in the  $\gamma = 1$  case. In practice,  $\kappa$  is usually at least  $10^4 \sim 10^5$ , and we conclude that the loss is ill-conditioned.

The ill-conditionness has two important implications. First, as gradient descent converges at a rate of  $O(\kappa)$ ,<sup>2</sup> we see that the time required for learning is  $O(N^2)$  for the RG algorithm, quadratic in the problem size. In contrast, Q-learning requires  $O(N)$  time to learn as it straightforwardly propagates reward information from  $s_{N-1}$  to  $s_0$ . Therefore, the RG algorithm is less efficient than Q-learning. It seems that this argument does not only apply to the RG algorithm and Q-learning, but also applies to gradient-TD and TD learning in general. Secondly, the ill-conditionness property implies that a small  $L_{MSBE}$  does not necessarily correspond to a short distance between the learned  $Q$  and the optimal  $Q^*$ , which may explain why  $L_{MSBE}$  is not a useful indicator of performance (Geist et al., 2017).

**Cliff walking** By way of demonstration, we consider a tabular problem, the *cliff walking* task in Sutton and Barto (2018), as illustrated in Fig. 1. The agent starts at the lower left corner in the grid and can move into nearby blocks. If it enters a white block, it receives a reward  $-1$ ; if it enters a grey block which is the cliff, it receives a reward  $-100$  and the process terminates; if it enters the goal it terminates with a reward zero. To learn this task, we initialize  $Q$  for all state-action pairs to be zero, and we proceed by randomly sampling a state-action pair  $(s, a)$ , use it as  $(s_t, a_t)$  to find the next state  $s_{t+1}$ , and update  $Q$  via Eq. (3) which is the Q-table learning, or minimize the associated loss  $(Q_\theta(s_t, a_t) - r_t - \gamma \max_{a'} Q_\theta(s_{t+1}, a'))^2$  following the gradient, which is RG learning. As shown in Fig. 1, RG learns more slowly than Q-table learning, and as shown in the right plots, for a given value of  $L_{MSBE}$ , RG’s distance to the optimal solution  $Q^*$  is larger than that of Q-table learning, showing that Q-table learning finds  $Q^*$  more efficiently. We find that the distance to  $Q^*$  is indeed closely related to the quality of policy and RG produces a worse policy than Q-table learning. To investigate the dependence on the size of the problem, we consider a width of 10 of the system with  $\gamma = 0.9$ , and its doubled size—a width of 20 with  $\gamma = 0.95$ . The results are presented in the upper and the lower plots in Fig. 1. Notice that the agent learns by randomly sampling from the state-action space, and doubling the system size reduces the sampling efficiency by a factor of two. As we have

<sup>2</sup>Although in the deterministic case momentum can be used accelerate gradient descent to a convergence rate of  $O(\sqrt{\kappa})$ , it cannot straightforwardly be applied to stochastic gradient descent since it requires a large momentum factor  $(\frac{\sqrt{\kappa}-1}{\sqrt{\kappa}+1})^2$  (Polyak, 1964) which results in unacceptably large noise.

<sup>3</sup> $|Q - Q^*|^2$  is defined by  $\sum_{(s,a)} |Q(s, a) - Q^*(s, a)|^2$ , summed over all state-actions.

the learning time of Q-learning being linear and RG being quadratic in the deterministic case, here their learning time respectively becomes 4 times and 8 times for the double-sized system. We see that the experimental results approximately coincide with this prediction, and support our analysis.

### 3.2 Tendency of maintaining the average prediction

Even if the efficiency problem of the ill-conditionedness is solved, the update rule of the RG algorithm still has a serious problem which can lead to unsatisfactory learning behaviour. To demonstrate this, suppose a person observes a state transition from  $s_t$  to  $s_{t+1}$  with action  $a_t$  and a reward  $r_t > 0$ , and suppose he/she did not expect the reward to appear, i.e. he/she predicted  $Q(s_t, a_t) = \gamma \max_{a'} Q(s_{t+1}, a')$ . Then after observing  $r_t$ , intuitively he/she will increase  $Q(s_t, a_t)$  exactly by an amount of  $r_t$ . This is because there is no evidence observed to support a change of  $Q(s_{t+1}, a')$  and  $Q(s_{t+1}, a')$  is kept fixed, which means that only  $Q(s_t, a_t)$  changes to accommodate the occurrence of  $r_t$  so that the Bellman equation is still satisfied. Therefore the average of  $Q(s_t, a_t)$  and  $Q(s_{t+1}, a')$  increases following the observation of  $r_t$ . To formulate this, we denote  $Q_t \equiv Q(s_t, a_t)$  and  $Q_{t+1} \equiv \max_{a'} Q(s_{t+1}, a')$ , and given that they are initialized to satisfy  $Q_t = \gamma Q_{t+1}$ , with an observed reward  $r_t$ , repeatedly applying the Q-table learning rule in Eq. (3) leads to  $\Delta(Q_t + Q_{t+1}) = \Delta Q_t = r_t$ . On the other hand, in the case of RG, minimizing  $L_{MSBE}$  corresponds to the learning rule

$$\Delta Q(s_t, a_t) = \alpha \left( r_t + \gamma \max_{a'} Q(s_{t+1}, a') - Q(s_t, a_t) \right), \quad \Delta \max_{a'} Q(s_{t+1}, a') = -\gamma \Delta Q(s_t, a_t), \quad (8)$$

and therefore whenever  $Q_t$  is changed,  $Q_{t+1}$  changes as well. Thus in the above scenario it has

$$\Delta(Q_t + Q_{t+1}) = (1 - \gamma)r_t, \quad (9)$$

and as  $\gamma$  is close to 1,  $\Delta(Q_t + Q_{t+1})$  can be very small, which is different from the learning with human intuition. The main reason for this to occur is that there is an additional degree of freedom when one modifies  $Q_t$  and  $Q_{t+1}$  to satisfy the Bellman equation. Q-table learning keeps  $Q_{t+1}$  fixed, while RG minimizes  $(Q_t - r_t - \gamma Q_{t+1})^2$  using the gradient and keeps  $Q_t + \frac{1}{\gamma} Q_{t+1}$  fixed. For  $\gamma \approx 1$ , the average of  $Q$  for all states is mostly preserved, except for the transitions to terminal states.

Although this looks like an efficiency issue, it has important consequences on the learning dynamics. If the average of  $Q$  is initialized above that of  $Q^*$ , and if the transitions among the states can form loops, the learning time of RG additionally scales as  $O\left(\frac{1}{1-\gamma}\right)$  due to the loops, regardless of the problem size  $N$  from the perspective of the optimal policy. In the cliff walking task with width 10, Q-table learning has roughly the same learning time for different  $\gamma$ , while RG scales roughly as  $O\left(\frac{1}{1-\gamma}\right)$  and does not learn for  $\gamma = 1$ , as shown in Fig. 2. This occurs because the learned policy  $\arg\max_{a'} Q(s, a')$  in RG almost always prefers non-terminal states and goes into loops, since transitions to terminal states are associated with Q values below what the agent currently predicts on average, and therefore Eq. (9) dominates the learning dynamics of moving from  $Q$ 's average to  $Q^*$ 's average.

A more commonly encountered failure mode appears when  $Q$  is initialized below  $Q^*$ , in which case the agent is seemingly contented with a small amount of reward and refuses to consistently pursue more reward. This occurs because when an unexpected reward  $r_t$  is found during learning, according to the learning rule in Eq. (8),  $\max_{a'} Q(s_{t+1}, a')$  decreases simultaneously with the increase of  $Q(s_t, a_t)$ , and therefore the action of the policy at  $s_{t+1}$ , i.e.  $\arg\max_{a'} Q(s_{t+1}, a')$ , is perturbed, and it can change to a worse action that produces less reward, and as a result, the performance of the agent does not improve on the whole. Also as the average of  $Q$  is mostly preserved, with an increase of  $Q$  for some of the states,  $Q$  for other states can decrease significantly, and in those states the agent would regard any little-rewarding action to be well above its expectation and likely learn a little-rewarding policy. In such cases, the performance of RG crucially relies on the exploration strategy involved. An example is in Fig. 3, for which  $Q$  is initialized to be zero and the agent learns from observed transitions in an online manner following the  $\epsilon$ -greedy policy.<sup>4</sup> We see that while Q-table learning can solve the problem easily without the help of  $\epsilon$ , RG cannot find the optimal policy with  $\epsilon = 0$ , and it learns slowly and crucially relies on  $\epsilon$ . However, in practice and especially for large-scale problems, one cannot increase  $\epsilon$  easily without hurting the performance. Therefore, RG often faces difficulties in learning and performs worse than Q-learning methods in practice.

<sup>4</sup> $\epsilon$ -greedy means that for probability  $\epsilon$  a random action is used; otherwise  $\arg\max_{a'} Q(s, a')$  is used.

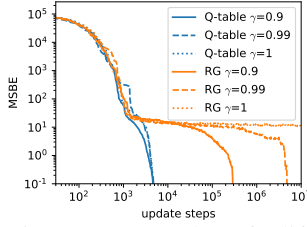


Figure 2: Results of cliff walking in Fig. 1 with different  $\gamma$ , with system’s width of 10, averaged over 10 runs. RG with  $\gamma = 1$  does not converge within reasonable computational budgets.

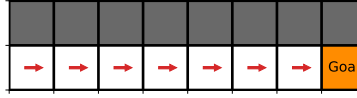
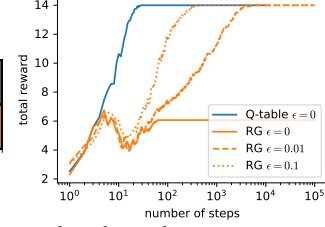


Figure 3: Left: one-way cliff walking task, where the agent starts at the lower left corner, and at each step it is allowed to move to the right to obtain a reward 2, or move up and terminate with a reward  $-1$ . It terminates when reaching the goal. Right: performance of the learned greedy policy for online Q-table learning and RG algorithm, following the  $\epsilon$ -greedy policy, for different values of  $\epsilon$ , with  $\gamma = 1$  and a learning rate of 0.5, averaged over 100 repeated runs.



**Remark** Although the above analysis is based on the tabular case, we believe that the situation is generally not better when function approximations are involved. With the above issues in mind, it can be understood why most of the currently successful examples of gradient-TD methods have tunable hyperparameters that can reduce the methods to conventional TD learning. When the methods get closer to conventional TD without divergence, they typically achieve better efficiency and better quality of the learned policy. When the agent only learns from the gradient of the loss without using tricks like target networks, the performance can be much worse. This probably explains why the performance of the PCL algorithm (Nachum et al., 2017) sometimes deteriorates when the value and the policy neural networks are combined into a unified Q network, and it has been reported that the performance of PCL can be improved by using a target network (Gao et al., 2018). Note that although ill-conditionedness can be resolved by a second order optimizer or the Retrace loss (Munos et al., 2016; Badia et al., 2020), the issue in Sec. 3.2 may not be resolved, because it will likely converge to the same optimum as the one found by gradient descent and have the same learning behaviour.

## 4 Convergent DQN algorithm

### 4.1 Interpreting DQN as fitted value iteration

As we find that Q-learning and the related conventional TD methods and DQN have learning behaviour preferable to RG, we wish to minimally modify DQN so that it can maintain its learning behaviour without non-convergence. Fortunately, this is possible. To proceed, we cast DQN into the form of fitted value iteration (FVI) (Munos and Szepesvári, 2008). With initial parameters  $\tilde{\theta}_0$  of the target network, the DQN loss for a transition  $(s_t, a_t, r_t, s_{t+1})$  and network parameters  $\theta$  can be defined as

$$\ell_{DQN}(\theta; \tilde{\theta}_i) := \left( Q_\theta(s_t, a_t) - r_t - \gamma \max_{a'} Q_{\tilde{\theta}_i}(s_{t+1}, a') \right)^2, \quad (10)$$

and DQN learns by iterating over the target networks

$$\tilde{\theta}_{i+1} = \underset{\theta}{\operatorname{argmin}} L_{DQN}(\theta; \tilde{\theta}_i), \quad L_{DQN}(\theta; \tilde{\theta}_i) := \mathbb{E} \left[ \ell_{DQN}(\theta; \tilde{\theta}_i) \right] \quad (11)$$

and  $\tilde{\theta}_i$  can be used as the trained network parameters given a sufficiently large  $i$ . In practice the minimum in Eq. (11) is approximately found by stochastic gradient descent. When DQN diverges, its loss is supposed to diverge with iterations, which means that we have  $\min_{\theta} L_{DQN}(\theta; \tilde{\theta}_{i+1}) > \min_{\theta} L_{DQN}(\theta; \tilde{\theta}_i)$  for some  $i$ .

### 4.2 Constructing a non-increasing series

Noticing that in DQN, at the moment when the target network  $\tilde{\theta}$  is copied from  $\theta$  we have  $L_{DQN}(\theta; \tilde{\theta}) = L_{MSBE}(\theta)$ , then if  $\min_{\theta} L_{DQN}(\theta; \tilde{\theta}_{i+1}) > \min_{\theta} L_{DQN}(\theta; \tilde{\theta}_i)$  is satisfied for some  $i$ , we have the following relation

$$\min_{\theta} L_{DQN}(\theta; \tilde{\theta}_i) < \min_{\theta} L_{DQN}(\theta; \tilde{\theta}_{i+1}) \leq L_{DQN}(\tilde{\theta}_{i+1}; \tilde{\theta}_{i+1}) = L_{MSBE}(\tilde{\theta}_{i+1}), \quad (12)$$

and therefore although  $\tilde{\theta}_{i+1}$  minimizes  $L_{DQN}(\theta; \tilde{\theta}_i)$ , it may increase  $L_{MSBE}(\theta)$ . Then we define our convergent DQN (C-DQN) loss as

$$L_{CDQN}(\theta; \tilde{\theta}_i) := \mathbb{E} \left[ \max \left\{ \ell_{DQN}(\theta; \tilde{\theta}_i), \ell_{MSBE}(\theta) \right\} \right], \quad (13)$$

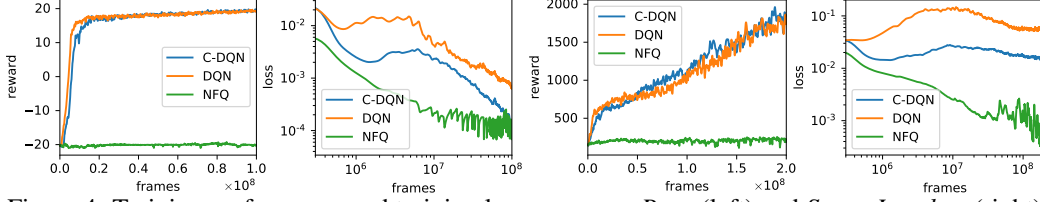


Figure 4: Training performance and training loss on games *Pong* (left) and *Space Invaders* (right).

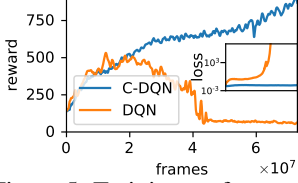


Figure 5: Training performance and training loss on *Space Invaders* when half of the data are randomly discarded.

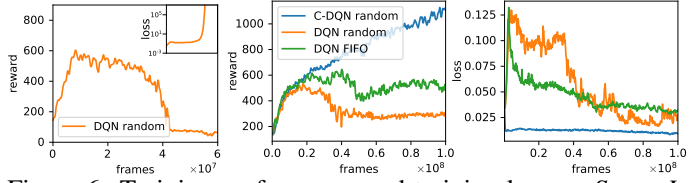


Figure 6: Training performance and training loss on *Space Invaders* when the memory adopts a random replacement strategy (left) and when the memory is smaller and adopts different strategies (middle and right).

with  $\ell_{MSBE}(\theta) := (Q_\theta(s_t, a_t) - r_t - \gamma \max_{a'} Q_\theta(s_{t+1}, a'))^2$ ,  $L_{MSBE} \equiv \mathbb{E}[\ell_{MSBE}]$ . Then we have

$$\min_{\theta} L_{CDQN}(\theta; \tilde{\theta}_{i+1}) \leq L_{CDQN}(\tilde{\theta}_{i+1}; \tilde{\theta}_{i+1}) = L_{MSBE}(\tilde{\theta}_{i+1}) \leq L_{CDQN}(\tilde{\theta}_{i+1}; \tilde{\theta}_i). \quad (14)$$

Similarly to DQN, we require that  $\tilde{\theta}_{i+1} = \operatorname{argmin}_{\theta} L_{CDQN}(\theta; \tilde{\theta}_i)$ , and we obtain the desired non-increasing condition

$$\min_{\theta} L_{CDQN}(\theta; \tilde{\theta}_{i+1}) \leq \min_{\theta} L_{CDQN}(\theta; \tilde{\theta}_i), \quad (15)$$

which implies that the iteration  $\tilde{\theta} \leftarrow \operatorname{argmin}_{\theta} L_{CDQN}(\theta; \tilde{\theta})$  is convergent, in the sense that the loss is lower-bounded and non-increasing.

C-DQN is convergent with a given fixed dataset, when the minima  $\tilde{\theta}_i$  are found precisely enough to reduce the loss. In practice, it suffices to simply replace the loss used in DQN by Eq. (13) to realize C-DQN. We empirically find that  $L_{MSBE}$  in RG is often reduced to a much smaller value than  $L_{DQN}$ , and therefore we expect C-DQN to focus on the DQN loss most of the time and to have learning behaviour similar to DQN. C-DQN can also be augmented by various extensions of DQN, such as double Q-learning, distributional DQN and soft Q-learning (Van Hasselt et al., 2016; Bellemare et al., 2017; Haarnoja et al., 2017), by modifying the losses  $\ell_{DQN}$  and  $\ell_{MSBE}$  accordingly. The mean squared loss can also be easily replaced by the Huber loss (smooth  $\ell_1$  loss) as commonly applied in DQN.

## 5 Experiments

### 5.1 Comparison of C-DQN, DQN and neural fitted Q iteration

We focus on the *Atari 2600* benchmark as in Mnih et al. (2015), and use the dueling network architecture and prioritized sampling, with double Q-learning where applicable (Wang et al., 2016; Schaul et al., 2015; Van Hasselt et al., 2016). We refer to the combination of the original DQN and these extensions simply as DQN, and similarly for C-DQN and neural fitted Q iteration (NFQ, which is essentially RG). Details of experimental settings are given in the supplemental material.

In order to stay close with established results, we follow the DQN hyperparameter settings in Hessel et al. (2018), and we show our results on two well-known games, *Pong* and *Space Invaders*. The training curves of performance and loss are presented in Fig. 4. We see that both C-DQN and DQN can learn the tasks, while NFQ almost does not learn, despite the fact that NFQ has its loss far smaller than the others. This coincides with our prediction in Sec. 3. We also find that C-DQN appears to learn slightly more slowly than DQN, which may be attributed to the DQN-favoring hyperparameters in the experiment. Overall, the results show that C-DQN as a theoretically convergent method indeed performs well in practice.

### 5.2 Learning from incomplete trajectories of experience

To show the divergence of DQN, we consider learning from incomplete trajectories of experience data, i.e. given a transition  $(s_t, a_t, s_{t+1})$  in the dataset, the transition  $(s_{t+1}, a_{t+1}, s_{t+2})$  may be absent from the dataset. We randomly discard half of the transition data collected by the agent and keep



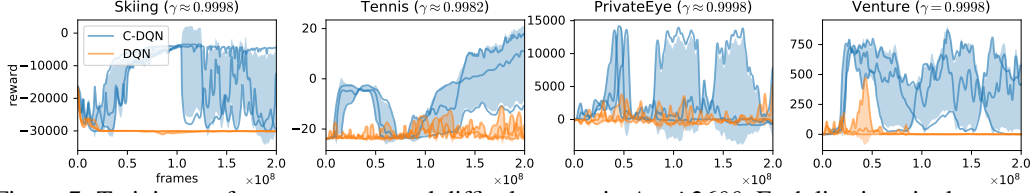


Figure 7: Training performance on several difficult games in *Atari 2600*. Each line is a single run and the shaded regions show the standard deviation. The discount factors used are shown in the titles and all DQN agents have significant instabilities or divergence in loss.

other experimental settings unchanged, except that instead of the Huber loss, the mean squared error is used. We find that the diverging behaviour is task-dependent, and the results for *Space Invaders* are shown in Fig. 5. We see that C-DQN learns stably and has good performance while DQN diverges. This shows that C-DQN can be used to learn from any given transition data, and C-DQN is therefore suited for offline learning and learning from pure observation.

A similar situation naturally arises when one replaces old data in the replay memory (i.e. the dataset) randomly by new data when the memory is full, instead of using the first-in-first-out (FIFO) strategy. In Fig. 6, we see that conventional DQN can actually diverge in such a case. In existing DQN literature, the replacement strategy is often ignored, while here we see that it is an important detail that affects the results. In practice, FIFO is almost always used. However, FIFO makes the memory data less diverse and less informative, and increases the possibility of the policy’s oscillation due to co-evolution with the replay memory, and as a result, a large size of the replay memory is often needed. In Fig. 6, we show that when the size of the replay memory is reduced to 1/10, C-DQN can benefit from utilizing the random replacement strategy while DQN cannot, and therefore C-DQN is able to reach a higher performance. This opens up a new possibility of RL of only storing and learning important data to improve efficiency, which cannot be realized stably with DQN but is possible with C-DQN.

### 5.3 Difficult games in Atari 2600

In this section we consider tackling difficult games in *Atari 2600*. While DQN often becomes unstable when the discount factor  $\gamma$  gets increasingly close to 1, in principle, C-DQN works well with any  $\gamma$ . However, we find that in practice, a large  $\gamma$  does not always result in superior performance, because a large  $\gamma$  requires the agent to predict rewards that are in the distant future and are often irrelevant for deriving the optimal policy, and therefore it can reduce learning efficiency and increase noise. We also notice that when  $\gamma$  goes beyond 0.9999, the order of magnitude of  $(1 - \gamma)Q_\theta$  gets close to the intrinsic noise caused by the finite learning rate, and the learning sometimes stagnates. Therefore, we require  $\gamma$  to stay between 0.99 and 0.9998, and we use a simple heuristic algorithm to evaluate how frequent reward signals appear in a system so as to decide  $\gamma$  for each task. The algorithm is given in the supplemental material and our evaluated  $\gamma$  mostly lies between 0.996 and 0.9998. As we collect sample trajectories to evaluate  $\gamma$ , we also take this opportunity to evaluate the mean  $\mu$  of  $Q$  and the scale  $\sigma$  of the reward signal, and make our agent learn a normalized value  $\frac{Q - \mu}{\sigma}$  instead of the original  $Q$ . We do not clip the reward and we follow Pohlen et al. (2018) to make the neural network learn a transformed Q function, which squashes the original Q function roughly by the square root.

We find that with C-DQN and large  $\gamma$ , several difficult tasks which previously could not be solved by DQN within moderate computational budgets can now be solved, as shown in Fig. 7. Each curve was obtained by running for 2 days on a single machine using a single process and an Nvidia Titan RTX GPU. We find that especially for *Skiing*, *Private Eye* and *Venture*, the agent significantly benefits from the large  $\gamma$  and achieves a higher best performance during training, even though *Private Eye* and *Venture* are only partially observable tasks and are not fully learnable by the agent. The learning rate is set to be  $4 \times 10^{-5}$ . Detailed comparison with existing works, further experiments and details of the experimental settings are given in the supplemental material.

## 6 Related Works

The slow convergence of RG compared with TD methods has been shown in Schoknecht and Merke (2003). However, the authors did not discuss the scaling properties as discussed in Sec. 3.1. The  $O(N^2)$  scaling property can also be derived by considering specific examples of Markov chains, such as the “Hall” problem as pointed out in Baird (1995). The convergence property of RG-like algorithms has been analysed in Antos et al. (2008), assuming that the underlying Markov process



is  $\beta$ -mixing, i.e. it converges to a stable distribution exponentially fast. However, this assumption is often impractical, which may have underlain the discrepancy between the theoretical optimality bounds of RG and the experimental effectiveness. There is an improved version of NFQ proposed in Zhang et al. (2020), and RG has been applied in robotics in Johannink et al. (2019). Concerning DQN, there are many attempts to stabilize the learning, to remove the target network, and to use a larger  $\gamma$ . Pohlen et al. (2018) introduces a temporal consistency loss, which is a penalty term to reduce the difference between  $Q_\theta$  and  $Q_{\tilde{\theta}}$  on  $s_{t+1}$ . The authors showed that the resulting DQN algorithm can learn with  $\gamma = 0.999$ . A modified version of it is proposed in Ohnishi et al. (2019). Kim et al. (2019) and Bhatt et al. (2019) propose extensions for DQN and show that the resulting DQN variants can sometimes operate without a target network when properly tuned. Achiam et al. (2019) gives an analysis of the divergence and proposes to use a method similar to natural gradient descent to stabilize Q-learning. Recently, the strategy of using target networks in DQN has been shown to be useful for TD learning in general by Zhang et al. (2021). Some other works have been discussed in previous sections and we do not repeat them here.

## 7 Conclusion and future perspectives

We have discussed the inefficiency issues concerned with RG and gradient-TD methods, and addressed the long-standing problem of convergence in Q-learning by proposing our convergent DQN algorithm as a careful combination of DQN and RG, and we have demonstrated the effectiveness of C-DQN on the *Atari 2600* benchmark. With the stability of C-DQN, we can now consider the possibility of tuning  $\gamma$  freely without sacrificing the stability, and the possibility of only learning important transitions to improve efficiency. C-DQN can be used for offline learning such as learning from observations, and applied to difficult tasks for which DQN shows instability. It can also be combined with many other strategies that involve target networks and potentially improve their capability.

There are many outstanding issues concerning C-DQN. The loss used in C-DQN is non-smooth, and it is not clear how this affects the optimization and the learning behaviour. In our experiments this does not seem to be a problem, but further investigation is desired. It is also interesting to investigate its interplay with DQN extensions such as double Q-learning and distributional DQN, and especially, whether there are better strategies to prioritize the sampled experience data, as some of the data may contribute to the loss via the term  $\ell_{DQN}(\theta; \tilde{\theta}_i)$  while others via  $\ell_{MSBE}(\theta)$ . It is not clear whether our target network can be updated softly as in Lillicrap et al. (2015). The effect of optimizers on C-DQN also deserves investigation (Zhuang et al., 2020; Luo et al., 2019; Ziyin et al., 2020), and it would be desirable if we can extend C-DQN so that it learns stochastic transitions without bias.

## Acknowledgments and Disclosure of Funding

We gratefully thank Zongping Gong for helpful advice on the analysis of the condition number, and we thank Murao Mio for discussion on the work. This work was supported by KAKENHI Grant No. JP18H01145 from the Japan Society for the Promotion of Science. Zhikang T. Wang was supported by Global Science Graduate Course (GSGC) program of the University of Tokyo.

## References

- Achiam, J., Knight, E., and Abbeel, P. (2019). Towards characterizing divergence in deep q-learning. *arXiv preprint arXiv:1903.08894*.
- Antos, A., Szepesvári, C., and Munos, R. (2008). Learning near-optimal policies with bellman-residual minimization based fitted policy iteration and a single sample path. *Machine Learning*, 71(1):89–129.
- Badia, A. P., Piot, B., Kapturowski, S., Sprechmann, P., Vitvitskyi, A., Guo, Z. D., and Blundell, C. (2020). Agent57: Outperforming the atari human benchmark. In *International Conference on Machine Learning*, pages 507–517. PMLR.
- Baird, L. (1995). Residual algorithms: Reinforcement learning with function approximation. In *Machine Learning Proceedings 1995*, pages 30–37. Elsevier.
- Bellemare, M. G., Dabney, W., and Munos, R. (2017). A distributional perspective on reinforcement learning. In *International Conference on Machine Learning*, pages 449–458. PMLR.

- Bellemare, M. G., Naddaf, Y., Veness, J., and Bowling, M. (2013). The arcade learning environment: An evaluation platform for general agents. *Journal of Artificial Intelligence Research*, 47:253–279.
- Berner, C., Brockman, G., Chan, B., Cheung, V., Debiak, P., Dennison, C., Farhi, D., Fischer, Q., Hashme, S., Hesse, C., et al. (2019). Dota 2 with large scale deep reinforcement learning. *arXiv preprint arXiv:1912.06680*.
- Bhatnagar, S., Precup, D., Silver, D., Sutton, R. S., Maei, H., and Szepesvári, C. (2009). Convergent temporal-difference learning with arbitrary smooth function approximation. *Advances in neural information processing systems*, 22:1204–1212.
- Bhatt, A., Argus, M., Amiranashvili, A., and Brox, T. (2019). Crossnorm: Normalization for off-policy td reinforcement learning. *arXiv preprint arXiv:1902.05605*.
- Dai, B., Shaw, A., Li, L., Xiao, L., He, N., Liu, Z., Chen, J., and Song, L. (2018). Sbed: Convergent reinforcement learning with nonlinear function approximation. In *International Conference on Machine Learning*, pages 1125–1134. PMLR.
- Durugkar, I. and Stone, P. (2017). Td learning with constrained gradients. In *Proceedings of the Deep Reinforcement Learning Symposium, NIPS 2017*, Long Beach, CA, USA.
- Ecoffet, A., Huizinga, J., Lehman, J., Stanley, K. O., and Clune, J. (2021). First return, then explore. *Nature*, 590(7847):580–586.
- Feng, Y., Li, L., and Liu, Q. (2019). A kernel loss for solving the bellman equation. *arXiv preprint arXiv:1905.10506*.
- Fösel, T., Tighineanu, P., Weiss, T., and Marquardt, F. (2018). Reinforcement learning with neural networks for quantum feedback. *Physical Review X*, 8(3):031084.
- Fujimoto, S., Meger, D., and Precup, D. (2020). An equivalence between loss functions and non-uniform sampling in experience replay. *arXiv preprint arXiv:2007.06049*.
- Gao, Y., Xu, H., Lin, J., Yu, F., Levine, S., and Darrell, T. (2018). Reinforcement learning from imperfect demonstrations. *arXiv preprint arXiv:1802.05313*.
- Geist, M., Piot, B., and Pietquin, O. (2017). Is the bellman residual a bad proxy? In *Advances in Neural Information Processing Systems*, pages 3205–3214.
- Ghiassian, S., Patterson, A., Garg, S., Gupta, D., White, A., and White, M. (2020). Gradient temporal-difference learning with regularized corrections. In *International Conference on Machine Learning*, pages 3524–3534. PMLR.
- Haarnoja, T., Tang, H., Abbeel, P., and Levine, S. (2017). Reinforcement learning with deep energy-based policies. *arXiv preprint arXiv:1702.08165*.
- He, K., Zhang, X., Ren, S., and Sun, J. (2015). Delving deep into rectifiers: Surpassing human-level performance on imagenet classification. In *Proceedings of the IEEE international conference on computer vision*, pages 1026–1034.
- Hessel, M., Modayil, J., Van Hasselt, H., Schaul, T., Ostrovski, G., Dabney, W., Horgan, D., Piot, B., Azar, M., and Silver, D. (2018). Rainbow: Combining improvements in deep reinforcement learning. In *Thirty-Second AAAI Conference on Artificial Intelligence*.
- Johannink, T., Bahl, S., Nair, A., Luo, J., Kumar, A., Loskyll, M., Ojea, J. A., Solowjow, E., and Levine, S. (2019). Residual reinforcement learning for robot control. In *2019 International Conference on Robotics and Automation (ICRA)*, pages 6023–6029.
- Kim, S., Asadi, K., Littman, M., and Konidaris, G. (2019). Deepmellow: removing the need for a target network in deep q-learning. In *Proceedings of the Twenty Eighth International Joint Conference on Artificial Intelligence*.
- Kingma, D. P. and Ba, J. (2014). Adam: A method for stochastic optimization. *arXiv preprint arXiv:1412.6980*.

- Levine, S., Pastor, P., Krizhevsky, A., Ibarz, J., and Quillen, D. (2018). Learning hand-eye coordination for robotic grasping with deep learning and large-scale data collection. *The International Journal of Robotics Research*, 37(4-5):421–436.
- Lillicrap, T. P., Hunt, J. J., Pritzel, A., Heess, N., Erez, T., Tassa, Y., Silver, D., and Wierstra, D. (2015). Continuous control with deep reinforcement learning. *arXiv preprint arXiv:1509.02971*.
- Luo, L., Xiong, Y., Liu, Y., and Sun, X. (2019). Adaptive gradient methods with dynamic bound of learning rate. *arXiv preprint arXiv:1902.09843*.
- Machado, M. C., Bellemare, M. G., Talvitie, E., Veness, J., Hausknecht, M., and Bowling, M. (2018). Revisiting the arcade learning environment: Evaluation protocols and open problems for general agents. *Journal of Artificial Intelligence Research*, 61:523–562.
- Mnih, V., Kavukcuoglu, K., Silver, D., Rusu, A. A., Veness, J., Bellemare, M. G., Graves, A., Riedmiller, M., Fidjeland, A. K., Ostrovski, G., et al. (2015). Human-level control through deep reinforcement learning. *nature*, 518(7540):529–533.
- Munos, R., Stepleton, T., Harutyunyan, A., and Bellemare, M. G. (2016). Safe and efficient off-policy reinforcement learning. *arXiv preprint arXiv:1606.02647*.
- Munos, R. and Szepesvári, C. (2008). Finite-time bounds for fitted value iteration. *Journal of Machine Learning Research*, 9(27):815–857.
- Nachum, O., Norouzi, M., Xu, K., and Schuurmans, D. (2017). Bridging the gap between value and policy based reinforcement learning. In *Advances in Neural Information Processing Systems*, pages 2775–2785.
- Ohnishi, S., Uchibe, E., Yamaguchi, Y., Nakanishi, K., Yasui, Y., and Ishii, S. (2019). Constrained deep q-learning gradually approaching ordinary q-learning. *Frontiers in neurorobotics*, 13:103.
- Pohlen, T., Piot, B., Hester, T., Azar, M. G., Horgan, D., Budden, D., Barth-Maron, G., Van Hasselt, H., Quan, J., Večerík, M., et al. (2018). Observe and look further: Achieving consistent performance on atari. *arXiv preprint arXiv:1805.11593*.
- Polyak, B. T. (1964). Some methods of speeding up the convergence of iteration methods. *Ussr computational mathematics and mathematical physics*, 4(5):1–17.
- Riedmiller, M. (2005). Neural fitted q iteration—first experiences with a data efficient neural reinforcement learning method. In *European Conference on Machine Learning*, pages 317–328. Springer.
- Schaul, T., Quan, J., Antonoglou, I., and Silver, D. (2015). Prioritized experience replay. *arXiv preprint arXiv:1511.05952*.
- Schoknecht, R. and Merke, A. (2003). Td (0) converges provably faster than the residual gradient algorithm. In *Proceedings of the 20th International Conference on Machine Learning (ICML-03)*, pages 680–687.
- Sutton, R. S. and Barto, A. G. (2018). *Reinforcement learning: An introduction*. MIT press.
- Sutton, R. S., Maei, H. R., Precup, D., Bhatnagar, S., Silver, D., Szepesvári, C., and Wiewiora, E. (2009). Fast gradient-descent methods for temporal-difference learning with linear function approximation. In *Proceedings of the 26th Annual International Conference on Machine Learning*, pages 993–1000.
- Sutton, R. S., Szepesvári, C., and Maei, H. R. (2008). A convergent o (n) temporal-difference algorithm for off-policy learning with linear function approximation. In *NIPS*.
- Touati, A., Bacon, P.-L., Precup, D., and Vincent, P. (2018). Convergent tree backup and retrace with function approximation. In *International Conference on Machine Learning*, pages 4955–4964. PMLR.
- Tsitsiklis, J. N. and Van Roy, B. (1997). An analysis of temporal-difference learning with function approximation. *IEEE transactions on automatic control*, 42(5):674–690.

- Van Hasselt, H., Doron, Y., Strub, F., Hessel, M., Sonnerat, N., and Modayil, J. (2018). Deep reinforcement learning and the deadly triad. *arXiv preprint arXiv:1812.02648*.
- Van Hasselt, H., Guez, A., and Silver, D. (2016). Deep reinforcement learning with double q-learning. In *Proceedings of the AAAI Conference on Artificial Intelligence*, volume 30.
- Wang, Z., Schaul, T., Hessel, M., Hasselt, H., Lanctot, M., and Freitas, N. (2016). Dueling network architectures for deep reinforcement learning. In *International conference on machine learning*, pages 1995–2003. PMLR.
- Wang, Z. T., Ashida, Y., and Ueda, M. (2020). Deep reinforcement learning control of quantum cartpoles. *Physical Review Letters*, 125(10):100401.
- Watkins, C. J. C. H. (1989). Learning from delayed rewards.
- Zhang, S., Boehmer, W., and Whiteson, S. (2020). Deep residual reinforcement learning. In *Proceedings of the 19th International Conference on Autonomous Agents and MultiAgent Systems, AAMAS ’20*, page 1611–1619, Richland, SC. International Foundation for Autonomous Agents and Multiagent Systems.
- Zhang, S., Yao, H., and Whiteson, S. (2021). Breaking the deadly triad with a target network. *arXiv preprint arXiv:2101.08862*.
- Zhuang, J., Tang, T., Ding, Y., Tatikonda, S., Dvornek, N., Papademetris, X., and Duncan, J. S. (2020). Adabelief optimizer: Adapting stepsizes by the belief in observed gradients. *arXiv preprint arXiv:2010.07468*.
- Ziyin, L., Wang, Z. T., and Ueda, M. (2020). LaProp: Separating Momentum and Adaptivity in Adam. *arXiv e-prints*, page arXiv:2002.04839.

## A Additional results on Atari 2600

### A.1 More flexible update periods for the target network

As the C-DQN has a better convergence property, it allows for shorter update periods for the target network. Specifically, convergence of the C-DQN is guaranteed as long as the iteration of the target networks satisfies

$$L_{CDQN}(\tilde{\theta}_{i+2}; \tilde{\theta}_{i+1}) \leq L_{CDQN}(\tilde{\theta}_{i+1}; \tilde{\theta}_{i+1}), \quad (16)$$

i.e., every next target network that is found should reduce loss, from which we have

$$L_{CDQN}(\tilde{\theta}_{i+2}; \tilde{\theta}_{i+1}) \leq L_{CDQN}(\tilde{\theta}_{i+1}; \tilde{\theta}_{i+1}) = L_{MSBE}(\tilde{\theta}_{i+1}) \leq L_{CDQN}(\tilde{\theta}_{i+1}; \tilde{\theta}_i) \quad (17)$$

and therefore the convergence is obtained. In practice, an iteration step of the target networks is done by first setting  $\theta$  to be equal to  $\tilde{\theta}_i$ , then doing  $N_{\tilde{\theta}}$  iterations of gradient descent on  $\theta$  minimizing  $L_{CDQN}(\theta; \tilde{\theta}_i)$  or  $L_{DQN}(\theta; \tilde{\theta}_i)$ , and finally using  $\theta$  as the next target network  $\tilde{\theta}_{i+1}$ .  $N_{\tilde{\theta}}$  is often referred to as the update period of the target network. In previous works on DQN,  $N_{\tilde{\theta}}$  is set to be 2000 or 2500 (Hessel et al., 2018; Mnih et al., 2015), and DQN may experience instability for a too small  $N_{\tilde{\theta}}$ . However, we empirically find that for many of the tasks in *Atari 2600*,  $N_{\tilde{\theta}}$  can be reduced to 200 or even 20 without any instability for C-DQN. Therefore, we see that C-DQN requires less fine tuning on the hyperparameter  $N_{\tilde{\theta}}$  compared with DQN. As examples, the experimental results on *Space Invaders* and *Hero* are shown in Fig. 8, using the experimental settings in Sec. 5.1. We see that C-DQN has a generally higher performance compared to DQN when  $N_{\tilde{\theta}}$  becomes small, and the performance of DQN is sometimes unstable and is sensitive to the value of  $N_{\tilde{\theta}}$ .

### A.2 Test performance on difficult Atari games

In this section we report the test performance of the agents in Sec. 5.3 and compare with existing works. As the learned policy of the agents has large fluctuations in performance due to noise, local optima, and insufficient learning when the task is difficult, instead of using the agent and the end of training, we use the best-performing agent during training to evaluate the test performance.

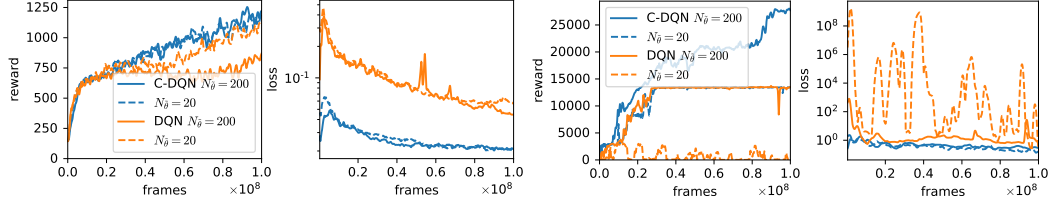


Figure 8: Training performance using different update periods of the target network on games *Space Invaders* (left) and *Hero* (right). In the game *Hero*, there appears to be a local optimum with reward 13000 where the learning can fail to make progress, which can also be seen in Fig. 12.

Table 1: Test performance on difficult *Atari 2600* games, corresponding to the results in Sec. 5.3 in the main text, evaluated using no-op starts and without using sticky actions (Machado et al., 2018), compared with other works. Human results and results for Agent57 are due to Badia et al. (2020), and results for Rainbow DQN are due to Hessel et al. (2018). The human results only represent the performance of an average person, not a human expert, and therefore the human results correspond to intuitively adequate performance in the games instead of the highest possible performance.

Task	C-DQN	DQN (Ours)	Human	Rainbow DQN	Agent57 (SOTA)
Skiing	<b>-3697 <math>\pm</math> 157</b>	-29751 $\pm$ 224	-4337	-12958	-4203 $\pm$ 608
Tennis	10.9 $\pm$ 6.3	-2.6 $\pm$ 1.4	-8.3	0.0	23.8 $\pm$ 0.1
Private Eye	14730 $\pm$ 37	7948 $\pm$ 749	69571	4234	79716 $\pm$ 29545
Venture	893 $\pm$ 51	386 $\pm$ 85	1188	5.5	2624 $\pm$ 442

Specifically, we save a checkpoint of the state  $\theta$  of the agent every  $10^4$  steps, and we choose the three best-performing agents by comparing their training performances, computed as the average of the 40 nearby episodes around each of the checkpoints. After the training, we carry out a separate validation process using 400 episodes to find the best-performing one among the three agents, and finally, we evaluate the test performance of the validated best agent by another 400 episodes, with a different random seed.<sup>5</sup> The policy during evaluation is the  $\epsilon$ -greedy strategy with  $\epsilon = 0.01$ , with no-op starts<sup>6</sup> (Mnih et al., 2015). The average of the test performances of the 3 runs in our experiments are shown in Table 1 with the standard error, compared with existing works and the human performance.

As we have mostly followed the conventional way of training DQN on *Atari 2600* as in Mnih et al. (2015) and Hessel et al. (2018), our C-DQN and the Rainbow DQN in Hessel et al. (2018) allow for a fair comparison as they use the same amount of computational budget and a similar neural network architecture.<sup>7</sup> In Table 1, we see that in these four difficult *Atari 2600* games where Rainbow DQN fails to make progress in learning, C-DQN can achieve performance higher than Rainbow DQN and have non-trivial learning. The results of Agent57 is for reference only. It represents the currently known best performance on *Atari 2600* in general and it does not allow for a fair comparison with C-DQN, because it involves considerably more computation, much more sophisticated techniques and larger neural networks. We find that the results on the game *Skiing* are exceptional and worth further discussion as done in the following subsection.

### A.3 The Atari game *Skiing*

In Table 1, one exceptional result is that our C-DQN achieves a performance higher than Agent57 on the game *Skiing*, using an amount of computation less than 0.1% of that of Agent57. In fact, we find that this performance is higher than any other known result so far and thus becomes a new state-of-the-art (SOTA) on this specific game. To elucidate the underlying reason, we describe this specific game first.

<sup>5</sup>We find that the policy of the agent during training often fluctuates dramatically, and a separate validation process is necessary in order to make sure that the agent involved in the evaluation of the test performance does not perform exceptionally.

<sup>6</sup>No-op starts mean that at the start of each episode the *no-operation* action is executed randomly for 1 to 30 frames.

<sup>7</sup>In fact, a fair comparison with Rainbow DQN can be made except for the case of *Skiing*, because reward clipping adopted by Rainbow DQN does not permit the learning of *Skiing*. Nevertheless, it does not affect our overall result.



Figure 9: A screenshot of the game *Skiing* in *Atari 2600*.

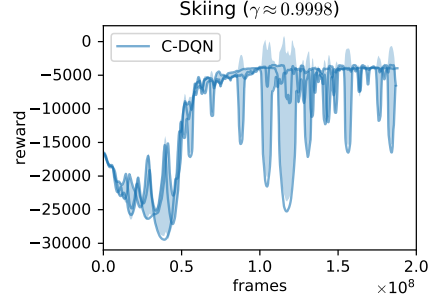


Figure 10: Training performance of C-DQN on *Skiing* with learning rate  $2 \times 10^{-5}$ , following the experimental procedure in Sec. 5.3. The standard deviation among the three runs are shown as the shaded region.

A screenshot of the game *Skiing* is shown in Fig. 9. The game is similar to a racing game. The player is required to go downhill and reach the goal as fast as possible, and the time elapsed before reaching the goal is the minus reward. At each time step, the player receives a small minus reward which represents the accumulated time, until the goal is reached and the game ends. In addition, the player is required to pass through the gates along his/her way, which are indicated by two small flags as in Fig. 9, and whenever the player fails to pass a gate, a 5-second penalty is added to the elapsed time when the player reaches the final goal. The number of gates that are yet to pass are shown at the top of the game screen. Using the standard setting in Mnih et al. (2015), the number of state transitions for an episode of this game is  $\sim 1300$  for the random policy,  $\sim 4500$  when the player slows down significantly, and  $\sim 500$  when the policy is near-optimal.

Since the penalty for not passing a gate is given only at the end of the game, the agent needs to relate the penalty at the end of the game to the events that happen early in the game, and therefore the discount factor  $\gamma$  should be at least as large as  $1 - \frac{1}{500}$  to make learning possible. However, the learning may still stagnate unless  $\gamma$  is even larger, because when  $\gamma$  is small, the agent prefers taking a longer time before reaching the goal, so that the penalty at the end is delayed and the Q function for states in the early game is increased, which will increase the episode length and make learning more difficult. Therefore, we have chosen to tune our hyperparameter setting so that  $\gamma \approx 1 - \frac{1}{5000}$  is obtained on this specific game (see Sec. B.3), and we find that our C-DQN agent successfully learns with the obtained  $\gamma$  and produces a new record on this game.<sup>8</sup> The large fluctuations in its performance during learning shown in Sec. 5.3 are mostly due to the noise coming from the finite learning rate, which can be confirmed by repeating the experiments with a smaller learning rate, shown in Fig. 10. However, in this case the learning easily gets trapped in local optima and the final performance is worse. Here, it is important to note that we cannot fairly compare our result with Agent57, because we have tuned the hyperparameters concerning  $\gamma$  in favour of this game,<sup>9</sup> while Agent57 uses a more general bandit algorithm to decide  $\gamma$ .

## B Experimental details on Atari 2600

### B.1 General settings

We follow Mnih et al. (2015) to preprocess the frames of the games by taking the maximum of the recent two frames and changing them to the grey scale. However, instead of downscaling them to  $84 \times 84$  images, we downscale exactly by a factor of 2, which results in  $80 \times 105$  images like done in Ecoffet et al. (2021). This is to preserve the sharpness of objects in the images and to preserve exact translational invariance of the objects. For each step of the agent, the agent stacks the frames seen in the recent 4 steps as the current observation, or as the state  $s_t$ , and decides an action  $a_t$  and executes the action repeatedly for 4 frames in the game and accumulates the reward in the 4 frames.

<sup>8</sup>The highest performance we observed was around  $-3350$ , and the optimal performance in this game is reported to be  $-3272$  in Badia et al. (2020).

<sup>9</sup>In our initial experiments, we find that with  $\gamma = 0.9998$ , sometimes DQN can also learn to perform well on *Skiing* with some specific training configurations. However, the result is much less general than that of C-DQN and we do not report it here.

Thus, the number of frames is 4 times the number of steps of the agent. One iteration of the gradient descent is performed for every 4 steps of the agent, and the agent executes the random policy for 50000 steps to collect some initial data before starting to do the gradient descent. The replay memory stores 1 million transition data, using the first-in-first-out strategy unless otherwise specified. The neural network architecture is the same as the one in Wang et al. (2016), except that we use additional zero padding of 2 pixels at the edges of the input at the first convolutional layer, so that all pixels in the  $80 \times 105$  images can be connected to the output. Similar to Hessel et al. (2018), we set the update period of target networks to be 8000 steps, i.e. 2000 gradient descent iterations, and we use the Adam optimizer (Kingma and Ba, 2014) with a mini-batch size of 32, and make the agent to regard the loss of one life in the game as the end of the episode. The default discount factor  $\gamma$  is set to be 0.99 unless otherwise specified, and the reward clipping to  $[-1, 1]$  is applied except in Sec. 5.3 and B.3.

**Gradient of  $L_{CDQN}$  when updating the target network** Although we use gradient descent to minimize  $L_{CDQN}$ , when we update the target network by copying from  $\theta$  to  $\tilde{\theta}$ , we have  $\ell_{DQN}(\theta; \tilde{\theta}_i)$  which is exactly equal to  $\ell_{MSBE}(\theta)$  and the gradient of  $L_{CDQN}$  is undefined. In this case, we find that one may simply use the gradient computed from  $\ell_{DQN}$  without any problem and rely on the later iterations to reduce the loss  $L_{CDQN}$ . In our experiments, we further avoid this issue by using the parameters  $\theta$  at the previous gradient descent step instead of the current step to update  $\tilde{\theta}$ , and therefore  $\theta$  does not become exactly equal to  $\tilde{\theta}$ . This strategy is valid because the consecutive gradient descent steps are supposed to produce parameters that minimize the loss almost equally well, and the parameters themselves should also be very close. In our implementation of DQN, we also update the target network in this manner to have a fair comparison with C-DQN.

**Loss** As mentioned in Sec. 4.2, either the mean squared error or the Huber loss can be used to compute the loss functions  $\ell_{DQN}$  and  $\ell_{MSBE}$ . In Sec. 5.2 we use one half of the mean squared error, and the loss functions are given by

$$\begin{aligned}\ell_{DQN}(\theta; \tilde{\theta}) &= \frac{1}{2} \left( Q_{\theta}(s_t, a_t) - r_t - \gamma \max_{a'} Q_{\tilde{\theta}}(s_{t+1}, a') \right)^2, \\ \ell_{MSBE}(\theta) &= \frac{1}{2} \left( Q_{\theta}(s_t, a_t) - r_t - \gamma \max_{a'} Q_{\theta}(s_{t+1}, a') \right)^2.\end{aligned}\tag{18}$$

In Sec. 5.1 we use the Huber loss, and the loss functions are given by

$$\begin{aligned}\ell_{DQN}(\theta; \tilde{\theta}) &= \ell_{Huber} \left( Q_{\theta}(s_t, a_t), r_t + \gamma \max_{a'} Q_{\tilde{\theta}}(s_{t+1}, a') \right), \\ \ell_{MSBE}(\theta) &= \ell_{Huber} \left( Q_{\theta}(s_t, a_t), r_t + \gamma \max_{a'} Q_{\theta}(s_{t+1}, a') \right), \\ \ell_{Huber}(x, y) &= \begin{cases} \frac{1}{2} (x - y)^2, & \text{if } |x - y| < 1, \\ |x - y| - \frac{1}{2}, & \text{if } |x - y| \geq 1. \end{cases}\end{aligned}\tag{19}$$

In Sec. 5.3, we let the agents learn a normalized Q function  $\hat{Q} \equiv \frac{Q - \mu}{\sigma}$ , and we use the strategy in Pohlen et al. (2018) to squash the Q function roughly by the square root before learning. The relevant transformation function  $\mathcal{T}$  is defined by

$$\mathcal{T}(\hat{Q}) := \text{sign}(\hat{Q}) \left( \sqrt{|\hat{Q}| + 1} - 1 \right) + \epsilon_{\mathcal{T}} \hat{Q},\tag{20}$$

and its inverse is given by

$$\mathcal{T}^{-1}(f) = \text{sign}(f) \left( \left( \frac{\sqrt{1 + 4\epsilon_{\mathcal{T}}(|f| + 1 + \epsilon_{\mathcal{T}})} - 1}{2\epsilon_{\mathcal{T}}} \right)^2 - 1 \right).\tag{21}$$

In our experiments we set  $\epsilon_{\mathcal{T}} = 0.01$  as in Pohlen et al. (2018). Our loss functions are then

$$\begin{aligned}\ell_{DQN}(\theta; \tilde{\theta}) &= \ell_{Huber} \left( f_{\theta}(s_t, a_t), \mathcal{T} \left( \hat{r}_t + \gamma \mathcal{T}^{-1} \left( \max_{a'} f_{\tilde{\theta}}(s_{t+1}, a') \right) \right) \right), \\ \ell_{MSBE}(\theta) &= \ell_{Huber} \left( f_{\theta}(s_t, a_t), \mathcal{T} \left( \hat{r}_t + \gamma \mathcal{T}^{-1} \left( \max_{a'} f_{\theta}(s_{t+1}, a') \right) \right) \right),\end{aligned}\tag{22}$$



where  $f_\theta$  is the neural network,  $\mathcal{T}^{-1}(f_\theta)$  is the learned normalized Q function  $\hat{Q}_\theta$ , and  $\hat{r}_t$  is the reward that is modified together with the normalization of the Q function, as discussed in Sec. B.3.

When we plot the figures, for consistency, we always report the mean squared error as the loss, given by

$$\begin{aligned}\ell_{DQN}(\theta; \tilde{\theta}) &= \left( Q_\theta(s_t, a_t) - r_t - \gamma \max_{a'} Q_{\tilde{\theta}}(s_{t+1}, a') \right)^2, \\ \ell_{MSBE}(\theta) &= \left( Q_\theta(s_t, a_t) - r_t - \gamma \max_{a'} Q_\theta(s_{t+1}, a') \right)^2,\end{aligned}\tag{23}$$

or,

$$\begin{aligned}\ell_{DQN}(\theta; \tilde{\theta}) &= \left( f_\theta(s_t, a_t) - \mathcal{T} \left( \hat{r}_t + \gamma \mathcal{T}^{-1} \left( \max_{a'} f_{\tilde{\theta}}(s_{t+1}, a') \right) \right) \right)^2, \\ \ell_{MSBE}(\theta) &= \left( f_\theta(s_t, a_t) - \mathcal{T} \left( \hat{r}_t + \gamma \mathcal{T}^{-1} \left( \max_{a'} f_\theta(s_{t+1}, a') \right) \right) \right)^2.\end{aligned}\tag{24}$$

As we have used double Q-learning (Van Hasselt et al., 2016) in our experiments, precisely speaking, all  $\max_{a'} Q_{\tilde{\theta}}(s_{t+1}, a')$  and  $\max_{a'} f_{\tilde{\theta}}(s_{t+1}, a')$  terms in the above equations are, in fact, replaced by  $Q_{\tilde{\theta}}(s_{t+1}, \arg\max_{a'} Q_\theta(s_{t+1}, a'))$  and  $f_{\tilde{\theta}}(s_{t+1}, \arg\max_{a'} f_\theta(s_{t+1}, a'))$ . These modifications do not change any of our arguments in Sec. 4, and they only make the optimization less smooth.

**Other details** We find that the exploration can often be insufficient when  $\gamma$  is large and when the game is difficult, and therefore we adopt a slightly more complicated schedule for the  $\epsilon$  parameter in the  $\epsilon$ -greedy policy. We have a total computation budget of  $5 \times 10^7$  steps for each agent. At the  $j$ -th step of the agent, for  $j \leq 50000$ , we have  $\epsilon = 1$  as the initial policy is random; for  $50000 > j \geq 10^6$ ,  $\epsilon$  is exponentially decreased to 0.1 following  $\epsilon = e^{j/\tau}$ , with  $\tau = 10^6 / \ln(0.1)$ ; for  $10^6 > j \geq 4 \times 10^7$ ,  $\epsilon$  is linearly decreased from 0.1 to 0.01; for  $j > 4 \times 10^7$  we set  $\epsilon = 0.01$ . This strategy makes  $\epsilon$  to stay above 0.01 for a fairly long time and facilitates exploration to reduce the effects of local optima. We use this  $\epsilon$  schedule in all of our experiments.

We set the learning rate to be  $6.25 \times 10^{-5}$  following Hessel et al. (2018) unless otherwise specified. We use gradient clipping in the gradient descent iterations, using the maximal  $\ell_2$  norm of 10 in Sec. 5.1 and 5.2, and of 5 in Sec. 5.3. The  $\epsilon_a$  hyperparameter for the Adam optimizer is set to be  $1.5 \times 10^{-4}$  in Sec. 5.2, and in Sec. 5.1 and A.1 it is set to be  $1.5 \times 10^{-4}$  for DQN,  $5 \times 10^{-5}$  for C-DQN, and  $5 \times 10^{-6}$  for NFQ, as we observe that the sizes of their gradients are different.  $\epsilon_a$  is set to be  $10^{-6}$  in Sec. 5.3 and B.3. The weight parameters in the neural networks are initialized following He et al. (2015), and the bias parameters are initialized to be zero.

## B.2 The prioritized sampling

In our experiments we have slightly modified the original prioritized sampling scheme. As proposed by Schaul et al. (2015), in the gradient descent, a transition data  $d_i = (s_t, a_t, r_t, s_{t+1}) \in \mathcal{S}$  is sampled with priority  $p_i$ , which is set to be

$$p_i = (|\delta_i| + \epsilon_p)^\alpha, \tag{25}$$

where  $\epsilon_p$  is a small positive number,  $\alpha$  is a sampling hyperparameter, and  $|\delta_i|$  is the evaluated Bellman error when  $d_i$  was sampled last time in gradient descent, which is

$$|\delta_{i(DQN)}| = \left| Q_\theta(s_t, a_t) - r_t - \gamma \max_{a'} Q_{\tilde{\theta}}(s_{t+1}, a') \right| \tag{26}$$

for DQN and

$$|\delta_{i(NFQ)}| = \left| Q_\theta(s_t, a_t) - r_t - \gamma \max_{a'} Q_\theta(s_{t+1}, a') \right|, \tag{27}$$

$$|\delta_{i(C-DQN)}| = \max \{ |\delta_{i(DQN)}|, |\delta_{i(NFQ)}| \}, \tag{28}$$

for NFQ and C-DQN, respectively. The probability for  $d_i$  to be sampled is  $P_i = \frac{p_i}{\sum_j p_j}$ . To correct the bias that results from prioritized sampling, an importance sampling weight  $w_i$  is multiplied to the loss computed on  $d_i$ , and it is given by

$$w_i = \left( \frac{\sum_j p_j}{N} \cdot \frac{1}{p_i} \right)^\beta, \tag{29}$$

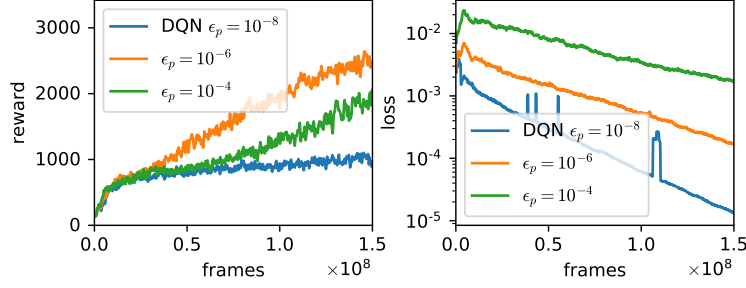


Figure 11: Training performance and loss for DQN on *Space Invaders*, with different hyperparameters  $\epsilon_p$  and following the prioritization scheme in Schaul et al. (2015). The loss is calculated by multiplying  $\tilde{w}_i$  and  $\ell_{DQN}$  on each sampled data.

where  $N$  is the total number of data and  $\beta$  is an importance sampling hyperparameter. The bias caused by prioritized sampling is fully corrected if  $\beta$  is set to be 1.

Schaul et al. (2015) propose using  $\tilde{w}_i := \frac{w_i}{\max_j w_j}$  instead of  $w_i$ , so that the importance sampling weight only reduces the size of the gradient. However, we find that this strategy would make the learning highly dependent on the hyperparameter  $\epsilon_p$  in Eq. (25), because given a vanishing  $|\delta_i|$ , we have the corresponding priority  $p_i \approx \epsilon_p^\alpha$  and therefore we have  $\max_j w_j = \left( \frac{\sum_j p_j}{N} \cdot \epsilon_p^{-\alpha} \right)^\beta \propto \epsilon_p^{-\alpha\beta}$ . As a result, the gradient in learning is scaled by the moving term  $\max_j w_j$  which is controlled by  $\alpha$ ,  $\beta$  and  $\epsilon_p$ . For a given  $\epsilon_a$  hyperparameter in the adaptive gradient descent optimizer, the overall decrease of the gradient caused by  $\max_j w_j$  is equivalent to an increase of  $\epsilon_a$ , which effectively anneals the size of update steps of the gradient descent throughout learning. This makes  $\epsilon_p$  an important learning hyperparameter, as also mentioned in Fujimoto et al. (2020), although this hyperparameter has been ignored in most of the existing works including the original proposal. The results on *Space Invaders* for different values of  $\epsilon_p$  are plotted in Fig. 11, which use the experimental settings in Sec. 5.1. We can see that the performance is strongly dependent on  $\epsilon_p$ . This issue may partially explain the difficulties one encounters when reproducing previous results.

**Lower bounded prioritization** To overcome this subtlety, we use the original importance sampling weight  $w_i$  instead of  $\tilde{w}_i$ . As  $|\delta_i|$  is heavily task-dependent, to remove the dependence of  $p_i$  on  $\epsilon_p$  for all the tasks, we use the average  $\bar{p} := \frac{\sum_j p_j}{N}$  to bound  $p_i$  from below instead of using  $\epsilon_p$ , which prevents  $p_i$  from vanishing. Specifically, we set  $p_i$  to be

$$p_i = \max \left\{ (|\delta_i| + \epsilon_p)^\alpha, \frac{\bar{p}}{\tilde{c}_p} \right\}, \quad (30)$$

where we set  $\epsilon_p$  to be a vanishing number  $10^{-10}$ , and  $\tilde{c}_p > 1$  is a prioritization hyperparameter that controls the lower bound relative to the average. In our experiments we set  $\tilde{c}_p = 10$ . This scheme makes sure that regardless of the size of  $|\delta_i|$ , a data is always sampled with a probability that is at least  $\frac{1}{\tilde{c}_p N}$ , and  $w_i$  is bounded by  $\tilde{c}_p^\beta$  from above, provided that  $\sum_j p_j$  does not change much. We adopt this prioritization scheme in all of our experiments, except for the experiments in Fig. 11 above. Compared to Fig. 4, it can be seen that our DQN loss and C-DQN loss on *Space Invaders* in Fig. 4 in the main text do not change as much.

**Details of setting** When a new data is put into the replay memory, it is assigned a priority that is equal to the maximum of all priorities  $p_i$  in the memory that have been calculated using Eq. (30), and at the beginning of learning when gradient descent has not started, we assign the collected data a priority equal to 100. We also additionally bound  $w_i$  from above by  $2\tilde{c}_p$ , so that  $w_i$  does not become too large even when the total priority  $\sum_j p_j$  fluctuates. The hyperparameter  $\beta$  is linearly increased from 0.4 to 1 during the  $5 \times 10^7$  steps of the agent, and  $\alpha$  is 0.9 in Sec. 5.3 and B.3 and is 0.6 otherwise. We did not try other values of  $\alpha$ .

In an attempt to improve efficiency, whenever we use  $|\delta_i|$  to update the priority  $p_i$  of a transition  $(s_t, a_t, r_t, s_{t+1})$ , we also use its half  $\frac{|\delta_i|}{2}$  to compute  $(\frac{|\delta_i|}{2} + \epsilon_p)^\alpha$ , and use it as a lower bound to update the priority of the preceding transition  $(s_{t-1}, a_{t-1}, r_{t-1}, s_t)$ . This strategy accelerates learning by

facilitating the propagation of information, and it is especially justified for  $\beta = 1$ , as the prioritization does not change the expected gradient. We have yet to fully investigate the effects of this strategy, but for most of the easy tasks in *Atari 2600* the effects are marginal. We use this strategy in all of our experiments except in Sec. 5.2, in order to make sure that the divergence shown in Sec. 5.2 is not due to this additional strategy.

### B.3 Evaluation of the discount factor and normalization of the learned Q function

**Evaluation of the discount factor** As discussed in Sec. A.3, certain tasks require a large discount factor  $\gamma$ . However for many other tasks, a large  $\gamma$  can slow down the learning significantly and make the optimization difficult. Therefore, we wish to find a method to automatically determine a suitable  $\gamma$  for a given task. As an attempt, we propose a heuristic algorithm to roughly estimate the frequency of the reward signal in an episode, based on which we can determine  $\gamma$ . The algorithm is described in the following.

Given an episode  $\mathcal{E}_k$  in the form of an ordered sequence of rewards  $\mathcal{E}_k = (r_i)_{i=0}^{T_k-1}$ , for which  $s_{T_k}$  is a terminal state,<sup>10</sup> we wish to have an estimate of the average number of steps needed to observe the next non-negligible reward if one starts from  $i = 0$  and goes to  $i = T_k$ . Suppose that all rewards  $\{r_i\}$  are either 0 or a constant  $r^{(1)} \neq 0$ ; then, we may simply count the average number of steps before seeing the next reward  $r^{(1)}$  when one moves from  $i = 0$  to  $T_k$ . However, such a strategy does not correctly respect the different kinds of distributions of the rewards in time, such as equispaced rewards and clustered rewards, and the strategy is symmetric with regard to the time reversal  $0 \leftrightarrow T_k$ , which is not satisfactory.<sup>11</sup> Therefore, we use a weighted average instead. To this end we define the return

$$R_i(\mathcal{E}_k) := \sum_{t=i}^{T_k-1} r_t, \quad (31)$$

which is the sum of rewards that are to be obtained starting from time step  $i$ , and we compute the average number of steps to see the next reward weighted by this return as

$$\hat{l}(\mathcal{E}_k) = \frac{\sum_{i=0}^{T_k-1} R_i(\mathcal{E}_k) l_i}{\sum_{i'=0}^{T_k-1} R_{i'}(\mathcal{E}_k)}, \quad l_i := \min\{t \mid t \geq i, r_t = r^{(1)}\} - i + 1 \quad (32)$$

where  $l_i$  is the number of steps to see the next reward starting from time step  $i$ . This strategy is not symmetric due to the introduction of  $R_i$ , and as the average is taken over the time steps, it distinguishes clustered rewards from equispaced rewards and it properly takes the distance between consecutive clusters of rewards into account.

The next problem is how we should deal with different magnitudes of rewards. As we can deal with the case of rewards being either 0 or constant, we may decompose a trajectory containing different magnitudes of rewards into a few sub-trajectories, each of which contains rewards that are either 0 or a constant, so that we can deal with each of these sub-trajectories using Eq. (32), and finally use a weighted average of  $\hat{l}$  over them as our result. With a set of episodes  $\{\mathcal{E}_k\}$ , we treat each of the episodes separately, and again, use a weighted average over the episodes as our estimate. The algorithm is given by Alg. 1. The weights in line 3 in Alg. 1 ensure that when computing the final result, episodes with a zero return can be properly ruled out, and that an episode with a large return does not contribute too much compared with the episodes with smaller returns. We have intentionally used the inverse in line 10 in Alg. 1 and used the root mean square in line 12 in order to put more emphasis on episodes that have frequent observations of rewards. Taking the absolute values of rewards in line 2 is customary, and in fact, one can also separate the negative and positive parts of rewards and treat them separately. Note that the output  $f$  should be divided by a factor of 2 to correctly represent the frequency of rewards. We also notice that the above approach can actually be generalized to the case of continuous variables of reward and time, for which integration can be used instead of decomposition and summation.

<sup>10</sup>We consider  $r_t$  to be the reward that is obtained when moving from state  $s_t$  to  $s_{t+1}$ .

<sup>11</sup>This is because if one almost sees no reward at the beginning but sees many rewards at the end of an episode, the time horizon for planning should be large; however, if one sees many rewards at the beginning but almost sees no reward at the end, the time horizon is not necessarily large. Note that a simple Fourier transform also respects the time reversal and thus does not suffice for our purposes.

---

**Algorithm 1** Estimation of the expected frequency of seeing a next reward signal

---

**Input:** sample episodes  $\{\mathcal{E}_k\}$   
**Output:** an estimate of the inverse of the number of time steps  $f$

```

1: for  $\mathcal{E}_k \in \{\mathcal{E}_k\}$  do
2:    $\mathcal{E}_k = (r_i)_{i=0}^{T_k-1} \leftarrow (|r_i|)_{i=0}^{T_k-1}$   $\triangleright$  Taking the absolute value of reward
3:    $w_k \leftarrow \sqrt{R_0(\mathcal{E}_k)}$   $\triangleright$  For computing a weighted average over different episodes
4:    $j \leftarrow 0$ 
5:   while rewards  $\mathcal{E}_k = \{r_i\}_{i=0}^{T_k-1}$  are not all zero do
6:      $j \leftarrow j + 1$ 
7:      $\mathcal{E}_k^{(j)}, \mathcal{E}_k \leftarrow \text{DECOMPOSESEQUENCE}(\mathcal{E}_k)$ 
8:   end while
9:   Compute  $l_k \leftarrow \frac{\sum_j R_0(\mathcal{E}_k^{(j)}) \hat{l}(\mathcal{E}_k^{(j)})}{\sum_{j'} R_0(\mathcal{E}_k^{(j')})}$   $\triangleright$  Weighting the results by the contribution of the rewards
10:   $f_k \leftarrow \frac{1}{l_k}$ 
11: end for
12: Compute  $f \leftarrow \sqrt{\frac{\sum_k w_k f_k^2}{\sum_{k'} w_{k'}}$   $\triangleright$  We use RMS to have more emphasis on episodes with larger  $f_k$ 
13: return  $f$ 
14:
15: procedure DECOMPOSESEQUENCE( $\mathcal{E}$ )
16:    $r' \leftarrow \min\{r_i\}_{i=0}^{T-1} = \min \mathcal{E}$ 
17:    $\mathcal{E}' \leftarrow (r''_i)_{i=0}^{T-1}, \quad r''_i := \begin{cases} 0, & \text{if } r_i = 0 \\ r', & \text{otherwise} \end{cases}$ 
18:    $\mathcal{E} \leftarrow (r_i - r''_i)_{i=0}^{T-1}$ 
19:   return  $\mathcal{E}', \mathcal{E}$ 
20: end procedure

```

---

To obtain the discount factor  $\gamma$ , we set the time horizon to be  $\frac{\tilde{c}_\gamma}{f}$ , with a time-horizon hyperparameter  $\tilde{c}_\gamma$ , and then we set  $\gamma = 1 - \frac{f}{\tilde{c}_\gamma}$ . To make  $\gamma$  close to 0.9998 for the difficult games discussed in Sec. 5.3, we have set  $\tilde{c}_\gamma = 15$ . However, later we noticed that the agent actually learns more efficiently with a smaller  $\gamma$ , and  $\tilde{c}_\gamma$  may be set to range from 5 to 15. In Sec. 5.3,  $\tilde{c}_\gamma = 15$  is used, but in the following experiments we use  $\tilde{c}_\gamma = 10$ .

We make use of the complete episodes in the initial 50000 transitions collected at the beginning of learning to evaluate  $\gamma$ , and here we also regard the loss of a life in the game as the end of an episode. We clip the obtained  $\gamma$  so that it lies between 0.99 and 0.9998, and  $\gamma$  is directly set to be 0.9998 if no reward is observed.

**Normalization of the Q function** In addition to using the transformation function  $\mathcal{T}(\cdot)$  to squash the Q function as described in Eq. (20) and (22), we normalize the Q function by the scale of the reward since the tasks in *Atari 2600* have vastly different magnitudes of rewards. For an episode  $\mathcal{E}_k$ , the Q function, or the value function, as the discounted return in the episode is given by

$$Q_{i;k} = \sum_{t=i}^{T_k-1} \gamma^{t-i} r_t, \quad (33)$$

and we compute its mean  $\mu$  by taking the average of  $Q_{i;k}$  over all states in given sample episodes. The standard deviation of  $Q_{i;k}$ , however, has a dependence on  $\tilde{c}_\gamma$ . If we simply normalize  $Q_{i;k}$  by its standard deviation, the magnitude of the reward signal after normalization becomes dependent on the hyperparameter  $\tilde{c}_\gamma$ , which we wish to avoid. To obtain a normalization that is independent of  $\tilde{c}_\gamma$ , we first assume that rewards are i.i.d. variables with mean  $\mu_r$  and standard deviation  $\sigma_r$ . Focusing on the Q function at the initial states, i.e.  $Q_{0;k}$ , we have the relation

$$\mathbb{E}[Q_{0;k}] = \frac{1 - \gamma^{T_k}}{1 - \gamma} \mu_r, \quad (34)$$

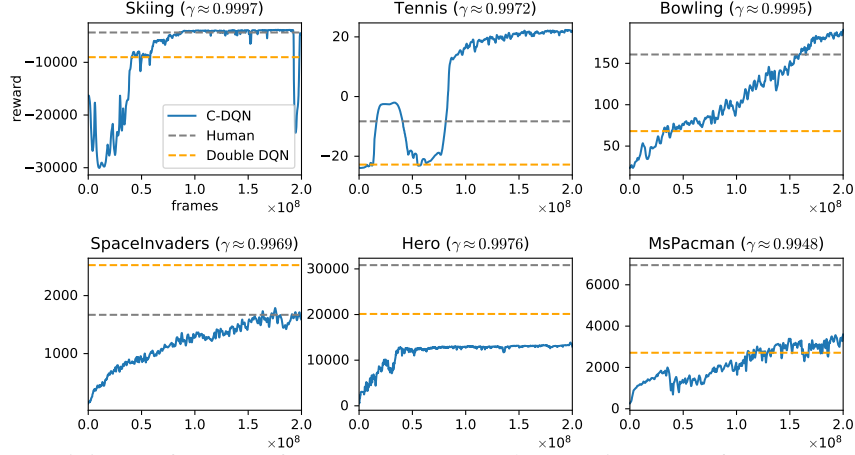


Figure 12: Training performance for C-DQN on several games in *Atari 2600* compared with the human performance (Badia et al., 2020) and the double DQN (Hessel et al., 2018), using the same experimental setting as in Sec. 5.3, except for using  $\tilde{c}_\gamma = 10$ .

and therefore we estimate  $\mu_r$  by  $\mu_r = \frac{1}{N_\mathcal{E}} \sum_k Q_{0;k} \frac{1-\gamma}{1-\gamma^{T_k}}$ , with the number of sample episodes  $N_\mathcal{E}$ . Also, we have

$$\text{Var} \left( Q_{0;k} - \frac{1-\gamma^{T_k}}{1-\gamma} \mu_r \right) = \frac{1-\gamma^{2T_k}}{1-\gamma^2} \sigma_r^2, \quad (35)$$

and therefore  $\sigma_r$  can be estimated by the variance of  $\left\{ \left( Q_{0;k} - \frac{1-\gamma^{T_k}}{1-\gamma} \mu_r \right) \cdot \sqrt{\frac{1-\gamma^2}{1-\gamma^{2T_k}}} \right\}_k$ .

To avoid the  $\tilde{c}_\gamma$  dependence, we use  $\sigma_r$  to roughly predict the standard deviation of  $Q_{0;k}$  when  $\gamma_0 \equiv 1 - \frac{f}{2}$  is used instead of the  $\tilde{c}_\gamma$ -dependent  $\gamma$  as the discount factor, and we use the obtained standard deviation as the normalization factor  $\sigma$ . For simplicity we ignore the variance of  $T_k$  and compute

$$\sigma = \sigma_r \cdot \frac{1}{N_\mathcal{E}} \sum_k \sqrt{\frac{1-\gamma_0^{2T_k}}{1-\gamma_0^2}}. \quad (36)$$

Finally, the function we let the agent learn is  $\hat{Q} \equiv \frac{Q-\mu}{\sigma}$ .

The normalized function  $\hat{Q}$  also obeys the Bellman equation, but with a slightly modified reward. It can be easily shown that

$$\hat{Q}^*(s_t, a_t) = \frac{r_t - (1-\gamma)\mu}{\sigma} + \gamma \max_{a'} \hat{Q}^*(s_{t+1}, a') \quad \text{if } s_{t+1} \text{ is non-terminal}, \quad (37)$$

and

$$\hat{Q}^*(s_t, a_t) = \frac{r_t - \mu}{\sigma} \quad \text{if } s_{t+1} \text{ is terminal}. \quad (38)$$

Therefore, the normalization amounts to modifying the reward  $r_t$  to  $\hat{r}_t := \frac{r_t - (1-\gamma)\mu}{\sigma}$ , and assigning an additional terminal reward  $-\frac{\gamma\mu}{\sigma}$ . This is easy to implement and we use this normalization strategy in our experiments. Similarly to the case of the evaluation of  $\gamma$ , we use the episodes in the initial 50000 transitions to compute  $\mu$  and  $\sigma$ ; however, here we do not regard the loss of a life as the end of an episode, so that the lengths of the episodes do not become too short. We also do not take episodes that have a zero return into account.

**Results on other Atari games** To demonstrate the general validity of the above strategy, we report our results on several games in *Atari 2600*, using a learning rate of  $4 \times 10^{-5}$  and  $\tilde{c}_\gamma = 10$ . The results are shown in Fig. 12. We find that for some games, especially *Hero*, the learning sometimes gets trapped in a local optimum and learning may stagnate, which deserves further investigation. We did not do a fine grid search on the learning rate and we only tried  $6 \times 10^{-5}$ ,  $4 \times 10^{-5}$  and  $2 \times 10^{-5}$ , and we chose  $4 \times 10^{-5}$ , because it produces reasonable results on most of the tasks. We notice that it is difficult to find a learning rate that works well for all the tasks, as the tasks have drastically different levels of stochasticity and are associated with different time horizons.

We also notice that there are several cases where our strategy for the normalization and the evaluation of  $\gamma$  does not produce satisfactory results. This is mainly because we have assumed that the time scales of obtaining rewards are similar for the random policy and for a learned policy. A typical counterexample is the game *Breakout*, where the random policy almost sees no reward in an episode but a learned policy frequently sees rewards. Therefore, our strategy above is still not general enough to deal with all kinds of scenarios, and it cannot replace the bandit algorithm in Badia et al. (2020) that has been used to select  $\gamma$ , and a better strategy is still desired.

## C Experimental details on cliff walking

In the cliff walking experiments, we store all state-action pairs into a table, excluding the states of goal positions and cliff positions, and excluding the actions that go into the walls. We plot the data on a log scale of iteration steps by explicitly evaluating the loss over all state-action pairs at different numbers of the iteration steps in Sec. 3.1, and evaluating the reward of the greedy policy in Sec. 3.2. Because we do evaluations at equal intervals on a log scale of the x-axis, fewer evaluations are made when the number of iteration steps becomes larger, and as a consequence, the scatter plots in the right of Fig. 1 do not have equally many data points along the curves. The learning rate  $\alpha$  is always 0.5, and  $\epsilon$  in the  $\epsilon$ -greedy policy is always fixed. Specifically for the one-way cliff walking task in Fig. 3, when two actions  $a_1$  and  $a_2$  have the same Q function value, i.e.  $Q(s_t, a_1) = Q(s_t, a_2)$ , the greedy policy randomly chooses  $a_1$  or  $a_2$  at state  $s_t$ , and when  $\max_{a'} Q(s_{t+1}, a') = Q(s_{t+1}, a_1) = Q(s_{t+1}, a_2)$ , we modify the learning rule of RG for transition  $(s_t, a_t, r_t, s_{t+1})$  to be

$$\begin{aligned}\Delta Q(s_t, a_t) &= \alpha \left( r_t + \gamma \max_{a'} Q(s_{t+1}, a') - Q(s_t, a_t) \right), \\ \Delta Q(s_{t+1}, a_1) &= \Delta Q(s_{t+1}, a_2) = -\frac{\gamma}{2} \Delta Q(s_t, a_t),\end{aligned}\tag{39}$$

so that the policy at  $s_{t+1}$  is not changed after learning from the transition.